Geodesy and Geodynamics 8 (2017) 59–69

Contents lists available at ScienceDirect

Geodesy and Geodynamics

journal homepages: www.keaipublishing.com/en/journals/geog; http://www.jgg09.com/jweb_ddcl_en/EN/volumn/home.shtml

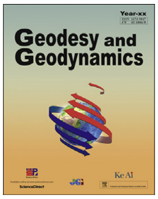

Multiplicity of solutions to geophysical inversion reflected by rupture slip distribution of the 2015 Nepal earthquake

Kai Tan [a], [*], Caihong Zhang [a], Bin Zhao [a], Qi Wang [b], Ruilin Du [a], Rui Zhang [c], Xuejun Qiao [a], Yong Huang [a]

[a] *Key Laboratory of Earthquake Geodesy, Institute of Seismology, China Earthquake Administration, Wuhan, 430071, China*
[b] *Institute of Geophysics and Geomatics, China University of Geosciences, Wuhan, 430074, China*
[c] *National Earthquake Infrastructure Service, Beijing, 100036, China*

ARTICLE INFO

Article history:
Received 10 October 2016
Accepted 22 December 2016
Available online 26 January 2017

Keywords:
Multiplicity of inversion solutions
Nepal earthquake
Coseismic deformation
Rupture slip distribution

ABSTRACT

The equivalence of geophysical fields, the finiteness of measurements and the measurement errors make the result of geophysical inversion non-unique. For example, the measurements and inversion method used, the priori rupture model determined and the slip distribution smoothing factor selected will have significant influences on the earthquake rupture slip distribution. Using different data and methods, different authors have given different rupture slip distribution models of the 2015 *M*w7.9 Nepal earthquake, with the maximum slip ranging from 3.0 m to 6.8 m. In this paper, geometry parameters of the single rectangular fault model in elastic half-space were inferred constraining with the Global Positioning System (GPS) and Interferometric Synthetic Aperture Radar (InSAR) coseismic deformations and bounding the slip with approximate average value; and then, the single rectangular fault was divided into multiple sub-faults, and the final slip smoothing factor, the final slip distribution and the maximum slip were determined with the misfit–roughness tradeoff curve, the cross-validation sum of squares (CVSS) and the third-party observation data or indexes being comprehensively taken into account. The results show that, the rupture of the Nepal earthquake extended by over 100 km east by south. The maximum slip of the earthquake was about 6.5–6.7 m, and most of the slip is confined at depths of 8–20 km, consistent with the depth distribution of aftershocks. The method for reducing the multiplicity of solutions to rupture slip distribution in this paper was ever used in inversion of rupture slip distribution for the 2008 Wenchuan and 2013 Lushan earthquakes, and the third-party measurement – surface dislocation has very large effect on reducing the multiplicity of solutions to inversion of the Wenchuan earthquake. Other priori information or indicators, such as fault strike, dip, earthquake magnitude, seismic activity, Coulomb stress, and seismic period, can be used for beneficial validation of and comparison with inversion results.

1. Introduction

As early as in the late 1960s, geophysicist Backus and applied mathematician Gilbert from USA expounded in their famous BG inversion theory that the solution to an inversion problem is highly non-unique. The intrinsic equivalence of the geophysical fields, the discreteness and finiteness of measurements, and the errors included in the observation field and the influences of other field sources cause the multiplicity of solutions to geophysical inversion. In inversion of the rupture slip distribution of an earthquake, the measurements and inversion method used, the priori rupture model determined and the slip distribution smoothing factor selected will have significant influences on the final rupture slip distribution.

For the 2015 *M*w7.9 Nepal earthquake, different authors have given different rupture models using different data, a-priori models

---

[*] *Corresponding author.*
E-mail address: whgpstan@163.com (K. Tan).

Peer review under responsibility of Institute of Seismology, China Earthquake Administration.

http://dx.doi.org/10.1016/j.geog.2016.12.003

and methods, with the maximum slip of the main shock ranging from 3.0 m to 6.8 m. The maximum slip values given by United States Geological Survey (USGS), and Zhang et al. [1] constrained by far-field seismic wave data are generally less than 4 m, and they can be increased to over 5 m with the introduction of GPS-derived near-field deformations. Other results constrained by Global Positioning System (GPS) and Interferometric Synthetic Aperture Radar (InSAR) data are more than 6 m in general [2–4]. Since the rupture of the Nepal earthquake did not outcrop, it failed to conduct comparison or constraint for the inversion results based on the geological survey data. The phenomenon of the multiplicity of solutions to inversion result of the rupture slip distribution of an earthquake has been shown in the research efforts on the 2008 Wenchuan and 2013 Lushan earthquakes; nevertheless, the geological survey data of rupture of the Wenchuan earthquake has played a role in testing the reliability of the model.

In this paper, taking the Nepal earthquake for example, with reference to the results of our studies on the Wenchuan and Lushan earthquakes, we analyzed the influences of different measurements, inversion methods, initial models of earthquake rupture, and rupture smoothing conditions on the inversion results of rupture slip distribution; studied the considerations for the following issues to improve the reliability of inversion results: selection of measurements and inversion method, determination of the fault rupture geometry and the rupture smoothing conditions; and proposed that use of the third-party measurements or indicators is important to constraint and check of the inversion results, so as to provide reference for reducing the multiplicity of solutions to inversion of seismic rupture slip.

2. The Nepal earthquake deformation and inversion method

Nepal is located in the junction region between the Eurasian and Indian plates, and at the southern foot of the middle segment of the Himalaya Mountains, where Himalayan main frontal thrust fault, main boundary thrust fault and main central thrust fault, and southern Tibetan detachment fault system are distributed. While the Indian Plate thrust beneath the Himalaya Mountains along the NNE direction at a rate of approximately 40 mm/a, the crust of the Himalaya Mountains in the middle of Nepal had a shortening convergence rate of approximately 20 mm/a [5], absorbing about a half of the inter-plate convergence rate. Intense tectonic movement gestated frequent seismic activities. An earthquake above *M*w8 ever occurred in the western Nepal in 1505, and an *M*w7.8 earthquake and an *M*w8.2 earthquake struck the eastern Nepal in 1833 and in 1934 respectively [6]. According to the global earthquake catalog, the middle region of Nepal has lacked strong earthquakes for a long time since 1976. The 2015 *M*w7.9 earthquake occurred to the west of the epicenters of great earthquakes occurring in 1833 and 1934, filling the seismic gap within more than 100 km on the west of the previous two great earthquakes.

We collected data from 260 GPS reference stations all over China and 17 GPS regional stations in Tibet, which belong to the "Crustal Movement Observation Network of China" (CMONOC in short); at these regional stations, conventional observation was conducted before April 2015, and expedited postseismic survey was performed immediately, with data sampling rate of 30 s. The non-profit university-governed consortium (UNAVCO) published the data acquired at 14 GPS continuous stations in Nepal. These GPS data, together with the data acquired at the IGS stations, were processed using the GAMIT/GLOBK software, and the data processing method is shown in corresponding reference [7]. The distribution of GPS coseismic horizontal displacement followed the deformation characteristic of thrust rupture, with displacement vectors pointing to the epicenter from both southern and northern sides. The maximum coseismic displacement, 1.89 m, occurred at KKN4 station in Nepal, only 9.5 km from the Global Centroid Moment Tensor (Global CMT, GCMT) epicenter. Coseismic displacements of 1.3–1.5 m were observed at two stations, approximately 50 km from the epicenter, in Nepal. In the southern Tibet in China, the maximum GPS-derived displacement, 54.0 cm, was at J041 regional station in Nyalam County, adjacent to Nepal. The displacements were approximately 13–15 cm at two regional stations (J040 and J339) in Gyirong County, approximately 140 km from the epicenter. The displacements were approximately 2 cm at stations in Zhongba and Angren, approximately 243 km from the epicenter. The coseismic deformations were generally less than 5 mm at other stations, over 400 km from the epicenter. The GPS-derived coseismic deformations in continuous observation had root mean square errors generally within 2 mm, and the deformations in mobile observation had root mean square errors within 4 mm. Given the GPS observation conditions and the model errors, the weight of GPS horizontal deformation was determined as 2 times the root mean square error.

University of California, San Diego published the L-band InSAR coseismic deformation results obtained by 4-view ALOS-2 satellites of Japan [8], and the wide-swath InSAR data during the ascending pass from February 22 to May 3, 2015 (Fig. 1) had the largest coverage; in this paper, the results of such wide-swath InSAR detrended data were re-sampled using the quadtree method to obtain 4437 sampling points, and the maximum deformation in the Line of Sight (LOS) was approximately 1 m. The GPS-derived 3D deformation data were projected to the LOS, and then compared with the InSAR LOS deformation values; the difference between them was within 5 cm in Nepal, consistent with the nominal error of InSAR observation [9]; in the southern Tibet, in particular, in the northeast corner of the InSAR image, the differences between them were generally 7–10 cm, so the InSAR observation results were likely influenced by more error factors, or negatively affected by elimination of the trend term in post-treatment. Therefore, the data in a small area on the northeast corner of the InSAR image were separated from the data in other areas, and different parameters were used to estimate the influence of the error of data in the small area in subsequent inversion. All InSAR LOS measurements were weighted uniformly based on an error of 5 cm [9].

Assuming that the focal area is an elastic half-space, then the surface deformation caused by an earthquake can be calculated with an elastic discoloration model in a half-space [10], and it is primarily related to seven geometry parameters (length, width, depth, strike, dip, and horizontal coordinates) and slip parameters (strike slip, dip slip, and tensile component) of a fault; thus, the fault rupture parameters can be inverted from the coseismic deformation measurements as constraints. If it is assumed that a rupture consists of a few large-area faults, then the purpose of the inversion is to solve for the approximate geometry and averaged slip of the rupture. If the rupture is further divided into more sub-faults, then the purpose of the inversion is to obtain detailed rupture slip distribution. Both inversion methods should minimize misfits to the deformation measurements subjected to weighted constraints on the roughness of slip distribution, that is,

$$\|\boldsymbol{W}(\mathbf{G}\boldsymbol{s}-\boldsymbol{d})\|^2+\beta^2\|\boldsymbol{Ls}\|^2=minimum \tag{1}$$

where $\boldsymbol{d}$ is the deformation measurement, including two horizontal components of GPS-derived displacement and the InSAR LOS deformation measurement. $\boldsymbol{W}$ is the weight matrix of measurements, which is the inverse matrix of the variance-covariance $\boldsymbol{D}$ of